Carbohydrate Research, 208 (1990) 215–230
Elsevier Science Publishers B.V., Amsterdam

Molecular structure of 3-*O*-(3,6-anhydro-α-D-galactopyranosyl)-β-D-galactopyranose (neocarrabiose) in the solid state and in solution: an investigation by X-ray crystallography, n.m.r. spectroscopy, and molecular mechanics calculations

Doriano Lamba, Anna Laura Segre,
Istituto di Strutturistica Chimica "Giordano Giacomello", Area della Ricerca di Roma, C.N.R., C.P. No. 10, 00016 Monterotondo Stanzione, Roma (Italy)

Steven Glover, William Mackie*, Bernard Sheldrick,
Astbury Department of Biophysics, University of Leeds, Leeds LS2 9JT (Great Britain)

and Serge Pérez
Laboratoire de Physicochimie des Macromolécules, Institut National de la Recherche Agronomique, B.P.527, 44026 Nantes 03 (France)

(Received January 24th, 1990; accepted for publication, April 6th, 1990)

ABSTRACT

The crystal structure of neocarrabiose monohydrate, 3-*O*-(3,6-anhydro-α-D-galactopyranosyl)-β-D-galactopyranose ($C_{12}H_{20}O_{10}\cdot H_2O$) belongs to the monoclinic space group $P2_1$, and has a unit cell of dimensions $a = 6.351(1)$, $b = 7.675(2)$, $c = 15.096(8)$ Å, and $\beta = 91.11(1)°$. The reducing unit is in the $^4C_1$ conformation, the non-reducing residue is $^1C_4$, with the 3,6-anhydro bridge in an *E* conformation, and HO-6 is in a *gauche–trans* conformation. The orientation about the (1→3) linkage is defined by $\varphi = 94.5°$ and $\psi = 141.9°$. There is an intramolecular hydrogen bond (O-5′···O-2 = 2.777Å). The conformations of the pyranose rings in solution, derived from $^3J_{H,H}$ values, were not significantly different from those in the crystal, but the 3,6-anhydro bridge assumed a half-chair conformation. All these features have been rationalised through molecular modelling and computation of potential energy surfaces.

INTRODUCTION

3-*O*-(3,6-Anhydro-α-D-galactopyranosyl)-D-galactopyranose (neocarrabiose) is a repeating unit of the carrageenans, a family of sulphated polysaccharides isolated from red algae[1]. The primary structures are based on alternate 3- and 4-linked β-D-galactopyranose residues. The principal differences arise from the occurrence of 4-linked 3,6-anhydro-D-galactopyranose or D-galactopyranose 6-sulphate (or 2,6-disulphate) residues as well as the distribution of sulphate groups elsewhere in the molecule, notably at position 4 of the 3-linked β-D-galactopyranose residues[1,2]. The ability of the carrageenans to form viscous solutions and hydrated gels, especially in association with group 1 cations, has found many applications, particularly in the food industries[3].

Carrageenans have been studied by polarimetry[4,5], n.m.r. spectroscopy[6–8], differ-

* Author for correspondence.

0008-6215/90/$03.50

ential scanning calorimetry[9], rheology[10], and X-ray fibre diffraction[11,12]. The last-mentioned studies showed that kappa- and iota-carrageenans adopt helical conformations that have three disaccharides in a repeat of ~25 Å. Furthermore, in iota-carrageenan, two identical polysaccharide chains are arranged to produce co-axial double helices. Subsequent studies of the calcium and strontium salts of iota-carrageenan by X-ray diffraction confirmed the double-helical structure, described such features as hydrogen bonding and cation co-ordination, and formed the basis of a molecular description of gel network formation in which double helices were an integral component of the junction zones.

An aim of the work now reported on neocarrabiose is part of a study of well-defined model compounds that was undertaken to provide precise details of structural factors (such as hydrogen bonding and cation co-ordination) which may be important in interactions at the polymer level.

EXPERIMENTAL

Nomenclature. — The conformation at the glycosidic linkage in neocarrabiose [**1**, 3-*O*-(3,6-anhydro-α-D-galactopyranosyl)-β-D-galactopyranose] is described by the torsional angles φ = O-5′–C-1′–O-3–C-3 or φ_H = H-1′–C-1′–O-3–C-3, and ψ = C-1′–O-3–C-3–C-4 or ψ_H = C-1′–O-3–C-3–H-3.

The orientation of the hydroxymethyl group is described by ω = O-5–C-5–C-6–O-6 and ω_H = H-5–C-5–C-6–O-6 and is referred[13] to as either *gauche–trans* (gt), *gauche–gauche* (gg), or *trans–gauche* (tg), corresponding to ω values of 60°, −60°, and 180°, respectively.

The orientation of the hydroxylic hydrogen atoms is described by Θ-i = HO-i–O-i–C-i–H-i.

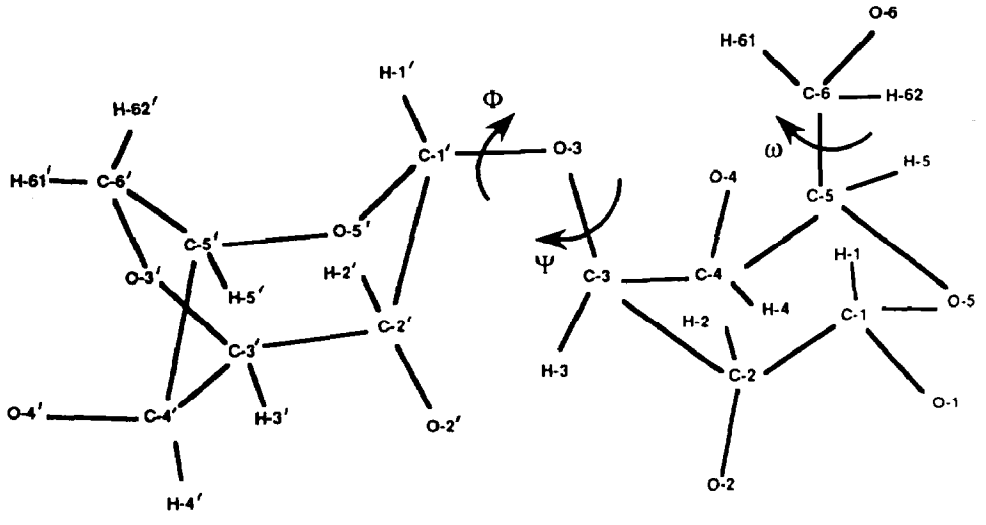

1

Crystallisation and X-ray investigation. — Neocarrabiose (Sigma), m.p. 164–166°, $[\alpha]_D^{24}$ +96°→ +111° (*c* 1.0, water) (literature values[14] m.p. 168–170°, $[\alpha]_D^{20}$ +85°→ +96°), was crystallised from water–propan-2-ol. Weissenberg photographs showed the space group to be $P2_1$ (monoclinic). A crystal (0.33 × 0.21 × 0.14 mm) in a Lindemann glass capillary was mounted on an Enraf–Nonius CAD-4F diffractometer for data collection. Unit cell parameters were determined from 18 measurements of Θ with $35° < \Theta < 43°$. The crystal data are given in Table I.

TABLE I

Crystal data for neocarrabiose

Molecular formula	$C_{12}H_{20}O_{10}\cdot H_2O$
Molecular weight	342.30
Crystal system	Monoclinic
Space group	$P2_1$
Cell dimensions	*a* (Å) 6.351(1), *b* (Å) 7.675(2), *c* (Å) 15.096(8), β (°) 91.11(1).
Cell volume (Å^3)	735.73
Z	2
F (000) (e)	364
μ(Cu-K$_\alpha$) (cm^{-1})	11.55
D_c (kg.dm^{-3})	1.545

Intensity data were collected in the $\omega-2\theta$ mode, using nickel-filtered Cu-K$_\alpha$ radiation up to $\theta = 70°$ for a total of 2993 reflections (h −7 to 7; k 0 to 9; l −18 to 18) of which 2749 were non-zero. A control reflection, 5 1 −5 was measured each hour of exposure time (83 measurements in all), with an average value of 623.3 counts and a standard deviation (of the distribution) of 20.3 (3.2%). Lorentz and polarisation corrections were applied, but no correction was made for absorption. The data were merged using the SHELX program[15] to give 1439 unique reflections, with a merging $R = 0.044$, of which 1439 with $F_o > 3\sigma(F_o)$ were used for the structural analysis.

The structure was solved by the direct methods program SHELX-84[16]. The E-map, computed for the phase set with the lowest combined figure of merit, showed all the non-hydrogen atoms, and the initial residual calculated for these atom positions was 0.193. The structure was refined isotropically ($R = 0.099$, unit weights) and then anisotropically, minimising the function $\Sigma\omega(|F_o| - |F_c|)^2$, where $\omega = 0.4101/\{\sigma_2(F_o) + 0.011050(F_o)^2\}$, together with anisotropic refinement of the overall scale factor. Subsequent difference Fourier syntheses revealed most of the hydrogen atoms attached to the pyranose rings, and those remaining were included in the later refinement in the positions calculated geometrically. The temperature factors of the hydrogen atoms were fixed with the equivalent U_{iso} values of the carrier atoms and some had their co-ordinates refined. The final R and R_w values were 0.046 and 0.067, respectively. In the final cycle of the refinement, the average shift/e.s.d. was 0.064. The final difference Fourier synthesis showed maximum and minimum electron densities of 0.20 and −0.30 eÅ^{-3}, respec-

TABLE II

Atom co-ordinates (× 10^4) and eqU_{iso} (× 10^4)

Atom	x/a	y/b	z/c	*eq*U_{iso}
C-1′	3702 (5)	8627 (6)	2713 (2)	342
C-2′	4704 (5)	10416 (6)	2574 (2)	354
C-3′	5894 (5)	10931 (6)	3432 (2)	380
C-4′	7605 (5)	9594 (6)	3612 (2)	381
C-5′	6226 (6)	8103 (6)	3910 (2)	421
C-6′	4739 (7)	9015 (7)	4524 (2)	528
O-2′	6205 (4)	10388 (5)	1877 (1)	433
O-3′	4474 (4)	10753 (6)	4155 (2)	527
O-4′	9005 (5)	10073 (6)	4312 (2)	547
O-5′	5146 (4)	7415 (5)	3130 (1)	411
C-1	−430 (5)	3997 (6)	1858 (2)	331
C-2	1664 (5)	4969 (5)	1954 (2)	333
C-3	1225 (5)	6921 (6)	1862 (2)	319
C-4	96 (5)	7314 (5)	980 (2)	313
C-5	−1893 (5)	6211 (5)	899 (2)	319
C-6	−2924 (5)	6427 (6)	−10 (2)	373
O-1	−92 (4)	2227 (5)	1894 (1)	395
O-2	2564 (4)	4558 (5)	2800 (1)	442
O-3	3128 (3)	7924 (5)	1895 (1)	362
O-4	1477 (3)	6932 (5)	277 (1)	373
O-5	−1359 (4)	4403 (5)	1007 (1)	339
O-6	−4819 (4)	5433 (−)	−122 (1)	417
W	−171 (5)	3463 (6)	4132 (2)	604

tively. The atomic scattering factors used were taken from the International Tables for X-Ray Crystallography[17]. The final atomic co-ordinates are listed in Table II*.

N.m.r. spectroscopy. — Spectra were recorded at 15° with a Bruker AM-200 spectrometer at 200.13 MHz on a solution (5 mg.mL^{-1}) of **1** in D_2O (internal acetone, 2.225 p.p.m.). The 2D-techniques LRCOSY and NOESY were applied for structural proof and conformational analysis. The following parameters were used.

1D ^{1}H-N.m.r. spectra: time domain, 16k; sweep width, 568 Hz corresponding to 0.069 Hz/point; 90° pulse; acquisition time, 14.4 s and no relaxation delay. The number of transients was 280. Resolution enhancement was achieved through a Gaussian multiplication before the Fourier transformation.

2D ^{1}H-N.m.r. spectra: size, 1k point in each dimension; the number of transients for each trace, 32; number of experiments, 256. Zero filling in the F1 dimension and sine bell multiplication for each dimension were performed before Fourier transformation. The contact time for NOESY was 300 ms and 1 s.

* The molecular geometry, vibrational parameters U_{ij} of the heavy atoms, the co-ordinates and U_{iso} values of the H atoms, a list of F_o and F_c structure factors, and Tables of bond lengths and angles are deposited with, and can be obtained from, Elsevier Science Publisher B.V., BBA Data Deposition, P.O. Box 1527, Amsterdam, The Netherlands. Reference should be made to No. BBA/DD/445/*Carbohydr. Res.* 208 (1990) 215–230.

Spectral analysis was performed with a modified version of the LACON3 type program[18] on a Data General Eclipse MV8000/II computer equipped with a digital Hewlett–Packard 7475A plotter. Each of the sugar units gives rise to a seven-spin system which was calculated separately. R.m.s. deviation between experimental and calculated spectra was <0.1 Hz for each residue. The two seven-spin systems were then added. The spectrum was simulated with a Lorentzian line-shape; a line-width of 0.30 Hz was assumed for all protons in both residues.

From the ^3J values, it is possible to derive reliable dihedral angles with the aid of the modified Karplus equation:
$^3J = \mathrm{P1}\cos^2 v + \mathrm{P2}\cos v + \mathrm{P3} + \Sigma \Delta X_i\,(\mathrm{P4} + \mathrm{P5}\cos^2\{\xi_1 v + \mathrm{P6}|\Delta X_i|\})$, where P1–P6 are the parameters given by Haasnoot *et al.*[19], ΔX_i = group electronegativity, ξ_1 = accounting for chirality (± 1), and v = dihedral angle.

Conformational analysis. — The allowed conformations and their energies were determined using separate computer programs of increasing complexity. The starting geometry was taken from the crystal structure of **1**.

(**a**) *Rigid map calculations.* For a given disaccharide, the conformational energy is evaluated by including the partitioned contributions arising from van der Waals interactions, torsional and exo-anomeric potential, and inter-residue hydrogen bonding, using the PFOS computer program[20,21]. The geometry of the ring is considered to be invariant and hydroxylic hydrogen atoms are not taken into account. For each of the three combinations of the orientation of the hydroxymethyl group, the torsional angles θ and ψ were increased in increments of 5° in the range $-180°$ to 180° and the calculations were performed with and without the contributions arising from hydrogen bonding[22]. The iso-contour levels were drawn at intervals of 1 kcal/mol with respect to the global minimum. The low-energy region was limited by the iso-energy contour corresponding to 10 kcal/mol above the minimum. Such maps are referred to as the rigid potential energy surfaces.

(*b*) *Relaxed map calculations.* Starting from the rigid potential surfaces in (*a*), a map was obtained in which every conformation was relaxed using the MM2CARB software[21], which is a version of the MM2 force field program[23] modified with the acetal fragment parameters from Jeffrey and Taylor[24]. The total energy takes into account the stretching, bending, stretch-bending, torsional, and dipolar contributions, and the van der Waals interactions. The hydrogen bond is not taken into account. The MM2CARB program reproduces, in an adequate fashion, the geometries of the rings and the linkages of the conformations observed in carbohydrates in the solid state[21]. For each of the three orientations of the hydroxymethyl group, the calculation was conducted as follows. Each of the local low-energy minima of the rigid potential energy surfaces was minimised through MM2CARB. Different orientations of the secondary hydroxyl groups, *i.e.* of all the Θ-i torsion angles, were tested in order to find the geometry with the lowest energy. Starting from these refined low-energy conformations, Φ and Ψ were set to the closest point in a 20° by 20° grid. Using the DRIVER option of the MM2 program, the conformational space was explored in a progressive way.

Packing analysis. — In order to arrive at a full description of the packing

arrangements, the intermolecular energy for the reference molecule and its neighbours was evaluated by taking into account the intermolecular hydrogen bonds and the non-bonded interactions. These calculations were performed using the same parameters as those in the conformational analysis of a single molecule [see (*a*) above]. The contributions to the energy were broken down into the non-bonded part and the intermolecular-hydrogen-bonding stabilisation. In addition, the number of short contacts corresponding to interatomic distances <1.5 times the sum of the van der Waals radii of the interacting atoms was computed.

RESULTS AND DISCUSSION

Molecular conformation in the solid state. — A representation (PLUTO[25]) of the asymmetric unit content of a neocarrabiose crystal is shown in Fig. 1. The present results establish that the conformation of the 3,6-anhydro-α-D-galactopyranose moiety is $^1C_4$, whereas that of the β-D-galactopyranose moiety is $^4C_1$. There was no evidence of any α,β configurational disorder at position 1 and there was one water molecule per disaccharide.

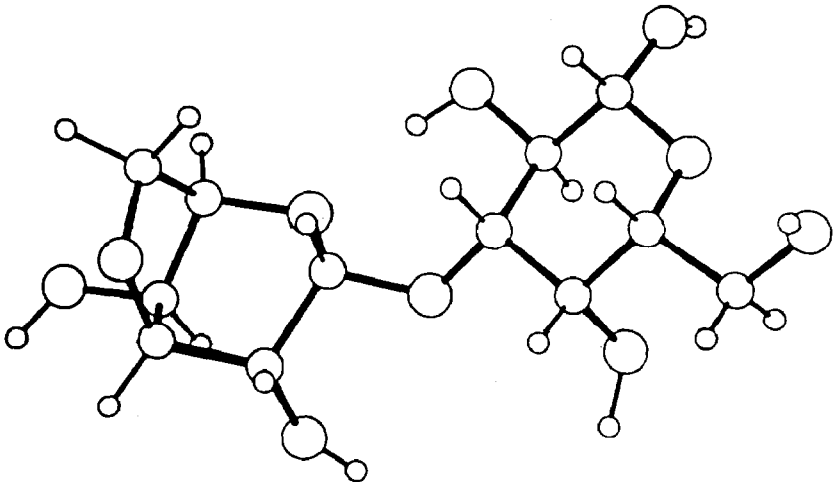

Fig. 1. PLUTO representation of the neocarrabiose (1) molecule in the crystal.

The mean C–C distances of 1.527(7) Å and the mean C–O bond length of 1.434(20) Å conform to the tabulated values of carbohydrates[26,27]. The anomeric bonds (1.393 and 1.383 Å, respectively) were in the normal range for equatorial linkages. With the exception of those involved in the 3,6-anhydro bridge, the internal C–C–C angles were close to tetrahedral [mean value, 109.2(1.2)°], whereas the exocyclic angle C-4–C-5–C-6 was slightly greater [110.8(3)°]. The exocyclic C–C–O angles averaged 110.2 (2.3)° for the 3,6-anhydrogalactose and 109.8(1.6)° for the galactose residue. The endocyclic C-5–O-5–C-1 angles varied little [average 113.8(2)°]. The glycosidic valence angle was 116.5° (Table III), which accords with that found[28] for the α-(1→3) linkage in

TABLE III

Geometry of the glycosidic linkage[a]

C-1′–O-3	1.393 (4)	C-3–O-3	1.439 (5)
C-1′–O-3–C-3	116.5 (2)		
O-5′–C-1′–O-3–C-3	94.5 (3)		
H-1′–C-1′–O-3–C-3	−23 (2)		
C-1′–O-3–C-3–C-4	141.9 (3)		
C-1′–O-3–C-3–H-3	20 (2)		

[a] Bond lengths (Å) and bond angles (°) with e.s.d.'s in parentheses.

TABLE IV

Puckering parameters of the pyranose rings and of the 3,6-anhydro bridge[a]

Parameter	*Reducing residue*	*Non-reducing residue*
Total puckering amplitude (Å)	0.592 (3)	0.669 (3) 0.452 (3)[a]
$\varphi 2$ (°)	108 (6)	122.0 (3) 99.8 (5)[a]
$\theta 2$ (°)	177.3 (3)	19.5 (2)
Minimum displacement	ΔC_s(C-4) 0.005 (2)	ΔC_s(C-4′) 0.003 (2)
Asymmetry parameter		ΔC_2(O-3′) 0.046 (1)
Conformation	$^4C_1$	$^1C_4$ E_4[a]
Displacement from the C-2–C-3–C-5–O-5 plane (Å)		
C-1	−0.71 (3)	0.57 (3)
C-4	0.68 (3)	−0.90 (3)
Displacement from the C-3′–C-5′–C-6′–O-3′ plane (Å)		
C-4′		−0.68 (3)

methyl α-nigeroside. Comparable values have been observed[29] for all linkage types except the (1→6) linkage.

The values of the ring puckering parameters[30] are given in Table IV. The expected $^4C_1$ (D) conformation was found for the β-D-galactopyranose residue, with no significant distortion from a perfect chair. The non-reducing residue adopted the $^1C_4$ (D) conformation and it exhibited some distortions. The 3,6-anhydro bridge was in an E_4 conformation with C-4′ displaced out of the least squares plane defined by C-3′, C-5′, C-6′, and O-3′ by 0.681 Å.

The primary hydroxyl group adopted a perfect gt conformation, which is one of the two preferred non-eclipsed orientations found in the solid state for monosaccharides having the *galacto* configuration[13].

The values of φ and ψ (Table III) for the (1→3) linkage in **1** were 94.5° and 141.9°, respectively, and this conformation was stabilised by an intramolecular hydrogen bond between O-2 and O-5′ of length 2.777 Å and of angle 167° (O-2–HO-2–O-5′).

Conformation in solution. — In the ^{1}H-n.m.r. spectrum of **1** (Fig. 2a), some of the resonances were split, giving rise to signal intensities that corresponded to less than one proton. This situation reflected the equilibrium of α and β anomers. Spectra measured on freshly prepared samples showed that the β anomer preponderated, but equilibrium was reached in <1 h. Fig. 2b, shows the calculated spectrum of the β anomer. The through-bond (scalar) coupling networks were traced by the ^{1}H–^{1}H LRCOSY proce-

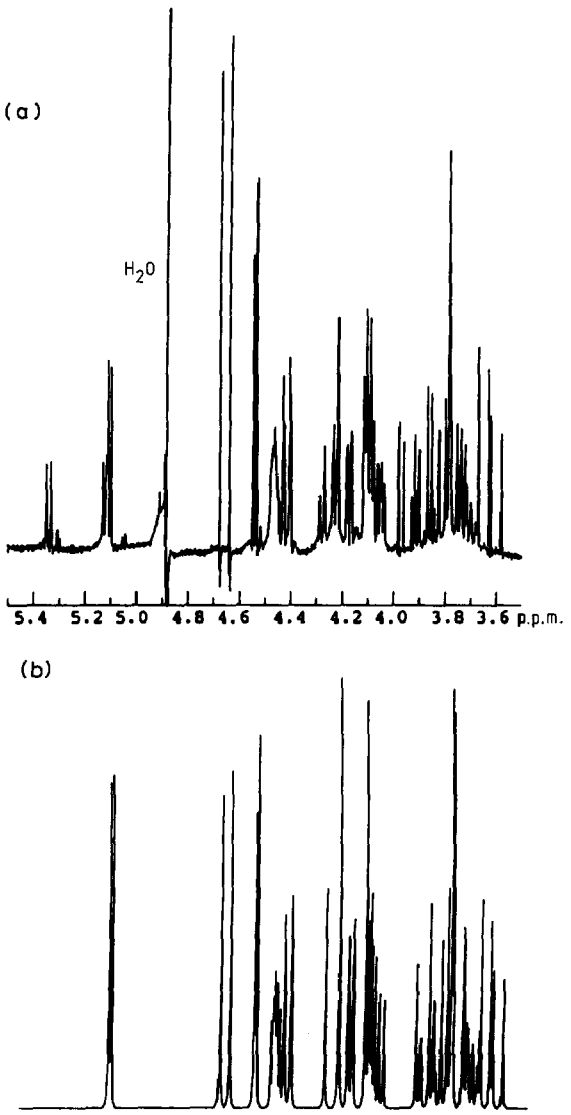

Fig. 2. ^{1}H-N.m.r. spectrum of neocarrabiose: (*a*) experimental, (*b*) calculated.

TABLE V

^{1}H chemical shifts (p.p.m.) obtained from spectral analysis and relative assignments

H-1'	*H-2'*	*H-3'*	*H-4'*	*H-5'*	*H-61'*	*H-62'*	
5.102	4.095	4.413	4.538	4.461	4.081	4.236	
H-1	*H-2*	*H-3*	*H-4*	*H-5*	*H-61*	*H-62*	
4.655	3.626	3.880	4.170	3.711	3.811	3.772	
^{3}J *values (Hz) obtained from spectral analysis*							
$J_{1',2'}$	$J_{2',3'}$	$J_{3',4'}$	$J_{3',5'}$	$J_{4',5'}$	$J_{5',61'}$	$J_{5',62'}$	$J_{61',62'}$
2.5	5.5	−0.2[a]	1.2	1.9	3.5	−0.2[a]	−10.7
$J_{1,2}$	$J_{2,3}$	$J_{3,4}$		$J_{4,5}$	$J_{5,61}$	$J_{5,62}$	$J_{61,62}$
7.9	9.9	3.4		0.9	7.9	4.4	−11.6

[a] Values within experimental error.

dure using the assignments for H-1 and H-1′ as a basis. ^{1}H chemical shifts and ^3J values are given in Table V.

The modified Karplus equation was used to compute the dihedral angles. Ambiguities in the equation, due to quadratic dependence on dihedral angles, can be removed by assuming that the conformation of the pyranose rings are the least distorted, with respect to an ideal $^4C_1$ or $^1C_4$ conformations, respectively. The H–C–C–H dihedral angles found in solution were similar to those observed for the crystal (Table VI). The only exception was the H-3′–C-3′–C-4′–H-4′ angle, since the small value of $J_{3,4}$ corresponded to the flat, poorly determined region close to $\pm 90°$ in the modified Karplus equation. The conformation of the rings of the β-D-galactopyranose and 3,6-anhydro-α-D-galactopyranose residues, in solution and in the crystal structure, were similar. The

TABLE VI

Dihedral angles (°) for **1** as derived from the crystal structure, n.m.r. experiments, and molecular mechanics calculations

3,6-Anhydro-α-D-galactopyranose *Angle*	*Crystal*	*N.m.r.*	*MM2CARB*
H-1′–C-1′–C-2′–H-2′	−39	−44	−48
H-2′–C-2′–C-3′–H-3′	−68	−50	−52
H-3′–C-3′–C-4′–H-4′	−69	−94/−80	−77
H-4′–C-4′–C-5′–H-5′	70	76	69
H-5′–C-5′–C-6′–H-61′	−85	−54	−81
H-5′–C-5′–C-6′–H-62′	40	72	42
β-D-Galactopyranose			
H-1–C-1–C-2–H-2	176	180	171
H-2–C-2–C-3–H-3	−168	−177	−170
H-3–C-3–C-4–H-4	57	50	54
H-4–C-4–C-5–H-5	−54	−52	−63
H-5–C-5–C-6–H-61	60		60
H-5–C-5–C-6–H-62	−176		−180

conformation of the 3,6-anhydro bridge is indicated by the values of $J_{5',61'}$ and $J_{5',62'}$. In order to assign the resonance of H-61′ and H-62′, an n.O.e. 2D-map was obtained with a short contact time of 300 ms. In this situation, only short intra-ring distances yield n.O.e. signals. A strong n.O.e. signal between H-1′ and H-62′ indicated their close proximity. The modified Karplus equation showed that only one set of solutions for the angles H-5′–C-5′–C-6′–H-61′ (v) and H-5′–C-5′–C-6′–H-62′ (v') can give rise to a strong n.O.e. signal between H-62′ and H-1′. Consideration of the Fisher–Newman projections showed that the valence angle can be calculated as $v + v'$, which is close to 120°. This solution is acceptable, and it is reported in Table VI. Hence, based on the assumption of the occurrence of a single conformation of the ring in solution, it may be concluded that the 3,6-anhydro bridge assumes a half-chair conformation in contrast to the *E* conformation found in the crystal structure.

The conformation around the C-5–C-6 bond cannot be determined since the resonances of H-61 and H-62 have similar chemical shifts and the coupling constants indicate an equilibrium of several conformers.

Information concerning the conformation at the glycosidic linkage was obtained by constructing an n.O.e. 2D-map (Fig. 3) with a contact time of 1 s. A large n.O.e. value between H-1′ an H-3 was observed (~5% in the magnitude projection). This effect was only slightly weaker than those observed between H-3 and H-1, and between H-3 and H-5.

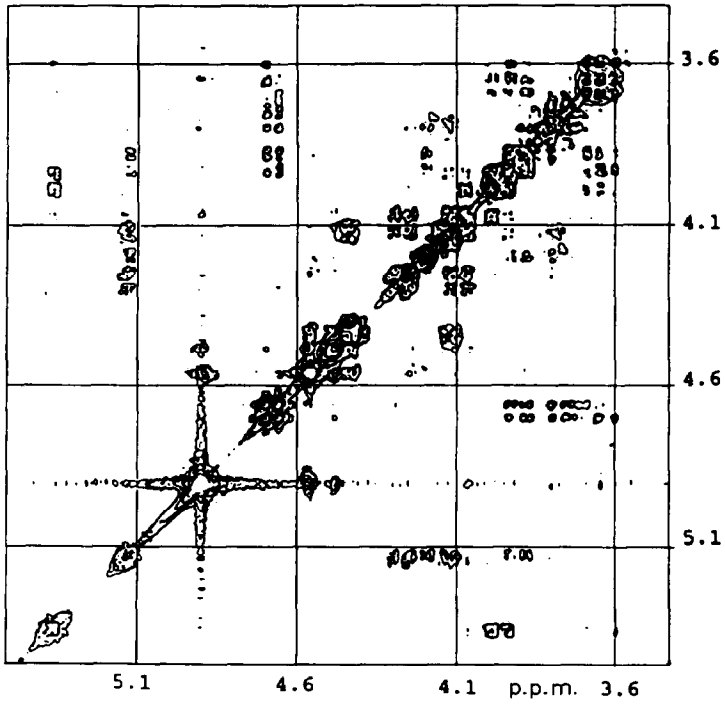

Fig. 3. NOESY spectrum of neocarrabiose.

Conformational analysis. — Initially, six rigid potential energy surfaces for the neocarrabiose molecule were computed that corresponded to the three possible non-eclipsed conformations about ω, both with and without the inclusion of an empirical hydrogen-bonding potential[22]. Comparison of these surfaces showed that the orientation about ω had no significant effect, and so, in the second stage, ω was allowed to remain at the MM2CARB value (174°). From a typical map, calculated without hydrogen bonds (Fig. 4), the values of φ and ψ for nine low-energy conformations can be determined (C1–C9); these are listed in Table VII in order of increasing energy, along

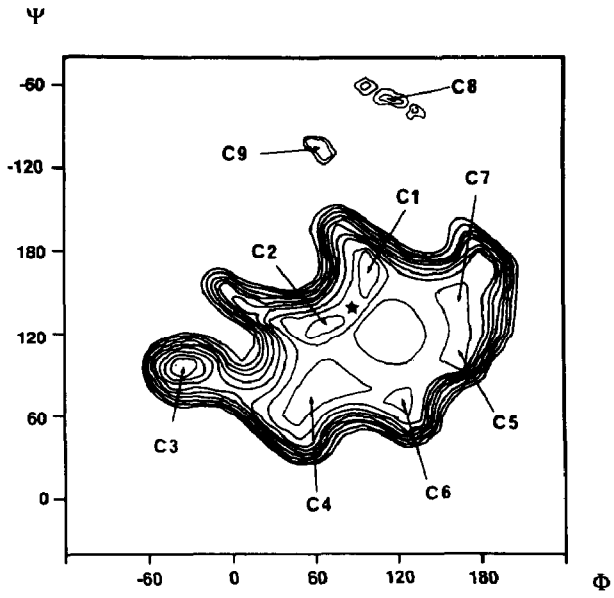

Fig. 4. Rigid potential energy surface of neocarrabiose, calculated with the crystal co-ordinates, with no incorporation of the hydrogen-bonding contribution. The iso-energy contours are drawn with interpolation of 1 kcal/mol above the minimum. The conformations of the nine stable conformers are located on the map.

TABLE VII

Summary of local minima[a], including selected distances (Å) from the crystal coordinates

	φ^o	ψ^o	E_{PFOS}	*O-5'–O-2*	*H-1'–H-3*	*H-1'–H-4*	*H-2'–H-3*	*H-3'–H-4*
Crystal	95	142	-	2.78	2.07	3.69	3.63	3.85
C1	100	170	−2.48	2.72	2.24	3.45	4.20	3.40
C2	80	130	−1.94	2.78	2.15	4.31	3.35	3.92
C3	−40	100	−1.94	-	3.56	4.61	3.71	3.57
C4	70	80	−1.00	-	2.70	4.45	2.13	4.36
C5	160	100	−0.87	-	2.20	4.25	3.55	2.66
C6	130	70	−0.77	-	2.29	3.42	2.36	3.70
C7	160	150	−0.75	-	2.49	3.35	4.37	2.21
C8	120	−70	3.84	-	3.27	1.68	4.14	3.62
C9	70	−110	6.38	-	3.55	1.98	4.00	4.50

[a] The energy is given in kcal/mol.

with some selected information on atomic distances. The nine energy minima fell into three classes. There were two "island" minima (C8 and C9) with energies of ~7 and 9 kcal/mol above the global minimum, and a central zone that contained the other seven minima, with energies ranging up to 3 kcal/mol above the global minimum. The crystal conformation was similar to C1 and C2 (the only ones with an intramolecular hydrogen bond), and all of these conformations are *prima facie* likely to occur in aqueous solution.

A typical "relaxed" map is presented in Fig. 5. Unlike Fig. 4, this φ,ψ map

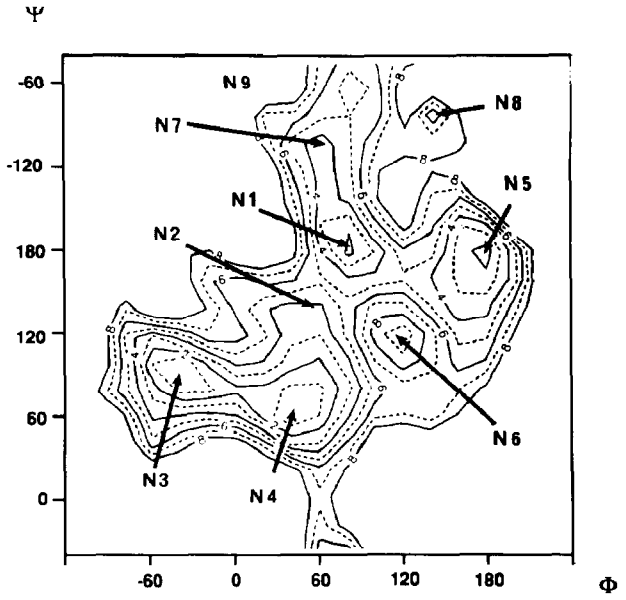

Fig. 5. Relaxed potential energy surface of neocarrabiose, calculated for a gt orientation of the primary hydroxyl group at the reducing residue. Iso-energy contours are drawn with interpolation of 1 kcal·mol^{-1} above the minimum of the map.

TABLE VIII

Summary of local minima[a], including selected distances (Å) from the MM2CARB-optimised coordinates

	Π	*π*	*E*	*O-5'–O-2*	*H-1'–H-3*	*H-1'–H-4*	*H-2'–H-3*	*H-3'–H-4*
N1	80	180	35.8	2.70	2.3	4.8	3.8	6.8
N2	60	140	37.6	2.72	2.2	3.4	4.2	6.6
N3	−40	90	34.5	-	3.5	3.5	3.7	6.1
N4	40	70	33.7	-	3.0	2.2	4.5	6.0
N5	180	190	37.5	-	3.2	4.6	2.3	6.6
N6	120	120	43.3	-	2.0	3.5	3.3	5.4
N7	60	−100	37.9	-	3.3	4.5	4.4	6.7
N8	140	−80	40.9	-	3.6	3.3	4.0	7.0
N9	80	−60	38.6	-	3.5	3.6	4.5	6.5

[a] The energy is given in kcal/mol.

represents a 2D projection of a multi-dimensional space, as the conformation is no longer a function of two variables but of many. The geometry of the nine low-energy conformations detected previously was refined completely. These local minima (N1–N9), along with selected distance information, are summarised in Table VIII.

The principal difference in gross outline of the two potential energy surfaces is fairly small, the C8 island having disappeared, and the C9 island having been joined to the "mainland", although there is still a substantial barrier of ~10 kcal/mol. Most of the minima found on the relaxed potential energy surface could be matched with their equivalents in the maps of the rigid potential energy surfaces, showing that the main effect of the MM2CARB optimisation was to improve the hydrogen positions that were responsible for a large number of poor contacts. The improvement in the locations of the hydrogen atoms upon MM2CARB optimisation was also apparent in the values of the H–C–C–H dihedral angles given in Table VI.

TABLE IX

Geometry of the hydrogen-bonding system

Donor-H···acceptor		*D···A (Å)*	*D–H (Å)*	*H···A (Å)*	*D–H···A (°)*
O-2-HO-2 ····· O-5′	(I)[a]	2.78	0.97	1.82	167
W-HW-2 ····· O-2	(I)	2.81	1.00	1.83	166
O-6-HO-6 ····· O-4	(I-a)	2.70	0.68	2.04	162
O-2′-HO-2′ ····· O-6	(II)	2.78	0.86	1.92	172
O-4-HO-4 ····· O-5	(II)	2.71	0.98	1.77	160
O-4′-HO-4′ ····· W	(I + a + b)	2.67	0.97	1.72	167
W-HW-1 ····· O-4′	(II + a + b)	2.74	0.94	1.81	169
Short contact					
O-2′ ····· O-1	(I + a + b)	2.74			

[a] Equivalent positions: (I) x, y, z; (II) $-x, \frac{1}{2}+y, -z$.

Hydrogen bonding and packing features. — The crystal structure **1** is stabilised by an extensive system of intermolecular hydrogen bonds described in Table IX. As already indicated, one intramolecular hydrogen bond occurred between O-2′ and O-5. There were six intermolecular hydrogen bonds per disaccharide molecule. Apart from O-2′, each oxygen atom was involved in two hydrogen bonds as acceptor and donor. A hydrogen bond was not formed between O-2′ and O-1 in spite of a separation of 2.74 Å, since the H···O distance is > 3 Å. The O-1 and O-3 were not involved in hydrogen bonds. The absence of hydrogen bonding to O-3 appears to be common to all di- and oligo-saccharides thus far characterised. The water molecule is involved in three hydrogen bonds, in two as donor and in one as acceptor. The network of some of these hydrogen bonds is shown in the (*b*,*c*) projection of the packing in Fig. 6.

The results obtained from a packing analysis of **1** are given in Table X. In the

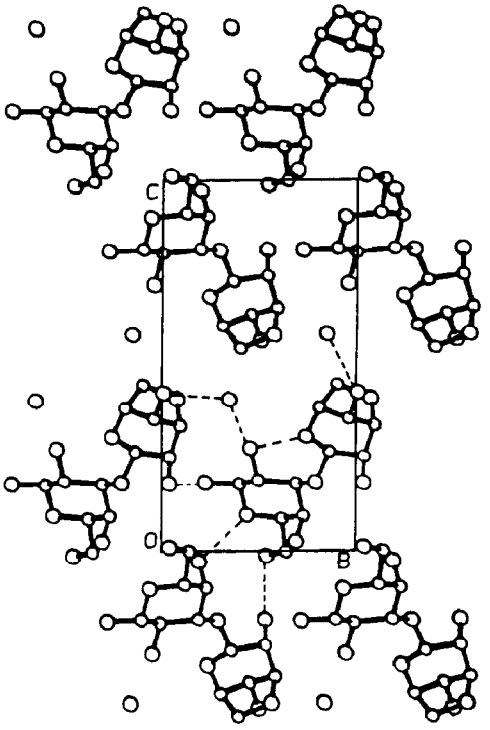

Fig. 6. Projected view (PLUTO) of the packing of neocarrabiose along the *a* axis. Some of the hydrogen bonds are shown as broken lines.

TABLE X

Packing features of neocarrabiose[a]

Molecule[b]	*Non-bonded energy (kcal/mol)*	*Intermolecular hydrogen bond (kcal/mol)*	*Total energy (kcal/mol)*	*Number of "short contacts"*
I−a/I + a	−5.28 (−5.14)	−1.72 (−1.72)	−7.00 (−6.86)	113 (110)
I + a + b/I−a−b	−1.71 (−1.16)	−1.51 (0.00)	−3.22 (−1.16)	33 (23)
I + b/I−b	−1.94 (−1.72)	0.00 (0.00)	−1.94 (−1.72)	35 (30)
II/II−b	−3.85 (−3.85)	−1.81 (−1.81)	−5.66 (−5.66)	74 (74)
II + a−b + c/II + a + c	−2.32 (−1.89)	−1.90 (0.00)	−4.22 (−1.89)	40 (40)
II−a/II−a−b	−0.73 (−0.73)	0.00 (0.00)	−0.73 (−0.73)	17 (17)
II + c/II−b + c	−0.29 (−0.29)	0.00 (0.00)	−0.29 (−0.29)	4 (4)
II + a/II + a−b	−0.10 (−0.10)	0.00 (0.00)	−0.10 (−0.10)	2 (2)

[a] The values obtained when the water molecules are omitted from the calculations are given in parentheses.
[b] Equivalent positions: (I) x, y, z; (II) $-x, \frac{1}{2} + y, -z$.

molecular arrangement in the crystal structure, the packing is dense, since each molecule of **1** is surrounded by 16 neighbours that occur in pairs, of which 4 had marginal contacts. The strongest layer, in terms of energy, arose from pure translational symmetry about the crystallographic axis *a*, and this could be correlated with the low value of the *a* axis of 6.531 Å. Another stable arrangement was achieved through a two-fold screw axis operation along the crystallographic axis *b*, that produced another type of "molecular chain". In this favourable arrangement, molecule I interacted with the one derived from the two-fold screw operation (molecule II) and with the translationally equivalent neighbours, *i.e.*, I + b and I − b. Such a strong molecular cohesion was reflected by the low value of the *b* axis (7.675 Å). The water molecule belonged to this molecular chain, but was not an essential component of the cohesive energy. However, the water participated, through hydrogen bonding, in the weak intermolecular associations along the *c* direction.

ACKNOWLEDGMENTS

We thank the N.m.r. Service of C.N.R. (Research Area of Rome), the University of Leeds Computing Service, and Centre de Recherches, I.N.R.A. (Nantes) for facilities. The provision of financial support by A.F.R.C. (to S.G.) and C.N.R. (to D.L.) is gratefully acknowledged. This work was supported in part by grants of the Italian National Research Council special *ad hoc* programme "Chimica Fine II" subproject 3 (to D.L. and A.L.S.).

REFERENCES

1 W. Mackie and R. D. Preston in W. D. P. Stewart (Ed.), *Algal Physiology and Biochemistry*, Blackwell, London, 1974, pp. 40–85.
2 T. J. Painter, in G. O. Aspinall (Ed.), *The Polysaccharides*, Vol. 2, Academic Press, London, 1983, pp. 202–285.
3 P. A. Sandford and J. Baird, in G. O. Aspinall (Ed.), *The Polysaccharides*, Vol. 2, Academic Press, London, 1983, pp. 411–490.
4 E. R. Morris, D. A. Rees, and G. Robinson, *J. Mol. Biol.*, 138 (1980) 349–362.
5 C. Rochas and S. Landry, *Carbohydr. Res.*, 7 (1987) 435–447.
6 P. S. Belton, G. R. Chilvers, V. J. Morris, and S. F. Tanner, *Int. J. Biol. Macromol.*, 6 (1984) 303–308.
7 P. S. Belton, V. J. Morris, and S. F. Tanner, *Int. J. Biol. Macromol.*, 7 (1985) 53–56.
8 G. P. Lewis, W. Derbyshire, S. Ablett, P. J. Lillford, and I. T. Norton, *Carbohydr. Res.*, 160 (1987) 397–410.
9 C. Rochas and M. Rinaudo, *Carbohydr. Res.*, 105 (1982) 227–236.
10 V. J. Morris and G. R. Chilvers, *Carbohydr. Polym.*, 3 (1983) 129–141.
11 S. Arnott, W. E. Scott, D. A. Rees, and C. G. A. McNab, *J. Mol. Biol.*, 90 (1974) 253–267.
12 R. P. Millane, R. Chandrasekaran, S. Arnott, and I. C. M. Dea, *Carbohydr. Res.*, 182 (1989) 1–17.
13 R. H. Marchessault and S. Perez, *Biopolymers*, 18 (1979) 2369–2374.
14 M. W. McClean and F. B. Williamson, in T. Levring (Ed.), *Proc. Int. Seaweed Symp., Xth*, de Gruyter, Berlin, 1981, pp. 479–484.
15 G. M. Sheldrick, *SHELX, Program for Crystal Structure Determination*, University of Cambridge, 1976.
16 G. M. Sheldrick, *Acta Crystallogr., Sect. A*, 40 (1984) c-440.
17 *International Tables for X-ray Crystallography*, Vol. 4, Kynoch Press, Birmingham, 1974.
18 S. Castellano and A. A. Bothner-By, *J. Chem. Phys.*, 41 (1964) 3863–3869.
19 C. A. G. Haasnoot, F. A. A. M. de Leeuw, and C. Altona, *Tetrahedron*, 36 (1980) 2783–2792.
20 S. Perez, D.Sc. Thesis, University of Grenoble, 1978.

21 I. Tvaroska and S. Perez, *Carbohydr. Res.*, 149 (1986) 389–410.
22 S. Perez and C. Vergelati, *Polym. Bull.*, 17 (1987) 141–148.
23 N. L. Allinger, *J. Am. Chem. Soc.*, 99 (1977) 8127–8134.
24 G. A. Jeffrey and R. Taylor, *J. Comp. Chem.*, 1 (1980) 99–109.
25 W. D. S. Motherwell and W. Clegg, *PLUTO-78, Program for Plotting Molecular and Crystal Structures*, University of Cambridge, 1978.
26 S. Arnott and W. E. Scott, *J. Chem. Soc., Perkin Trans. 2*, (1972) 324–335.
27 F. H. Allen, *Acta Crystallogr., Sect. B*, 42 (1986) 515–522.
28 A. Neuman, D. Avenel, F. Arene, H. Gillier-Pandraud, J. R. Pougny, and P. Sinaÿ, *Carbohydr. Res.*, 80 (1980) 15–24.
29 A. Imberty and S. Perez, *Carbohydr. Res.*, 181 (1988) 41–55.
30 D. Cremer and J. A. Pople, *J. Am. Chem. Soc.*, 97 (1975) 1354–1358.